

Curvature Graph Generative Adversarial Networks

Jianxin Li^{1,2}, Xingcheng Fu^{1,2}, Qingyun Sun^{1,2}, Cheng Ji^{1,2}, Jiajun Tan¹, Jia Wu³, Hao Peng¹

¹ Beijing Advanced Innovation Center for Big Data and Brain Computing, Beihang University, Beijing 100191, China

² School of Computer Science and Engineering, Beihang University, Beijing 100191, China

³ School of Computing, Macquarie University, Sydney, Australia

{lijx, fuxc, sunqy, jicheng, penghao}@act.buaa.edu.cn, chiachiun_than@buaa.edu.cn, jia.wu@mq.edu.au

ABSTRACT

Generative adversarial network (GAN) is widely used for generalized and robust learning on graph data. However, for non-Euclidean graph data, the existing GAN-based graph representation methods generate negative samples by random walk or traverse in discrete space, leading to the information loss of topological properties (e.g. hierarchy and circularity). Moreover, due to the topological heterogeneity (i.e., different densities across the graph structure) of graph data, they suffer from serious topological distortion problems. In this paper, we proposed a novel Curvature Graph Generative Adversarial Networks method, named **CurvGAN**, which is the first GAN-based graph representation method in the Riemannian geometric manifold. To better preserve the topological properties, we approximate the discrete structure as a continuous Riemannian geometric manifold and generate negative samples efficiently from the wrapped normal distribution. To deal with the topological heterogeneity, we leverage the Ricci curvature for local structures with different topological properties, obtaining to low-distortion representations. Extensive experiments show that CurvGAN consistently and significantly outperforms the state-of-the-art methods across multiple tasks and shows superior robustness and generalization.

CCS CONCEPTS

• **Computing methodologies** → **Neural networks; Learning latent representations**; • **Mathematics of computing** → **Graphs and surfaces**.

KEYWORDS

Graph representation learning, generative adversarial networks, Riemannian manifold, hyperbolic space, spherical space

ACM Reference Format:

Jianxin Li^{1,2}, Xingcheng Fu^{1,2}, Qingyun Sun^{1,2}, Cheng Ji^{1,2}, Jiajun Tan¹, Jia Wu³, Hao Peng¹. 2022. Curvature Graph Generative Adversarial Networks. In *Proceedings of the ACM Web Conference 2022 (WWW '22)*, April 25–29, 2022, Virtual Event, Lyon, France. ACM, New York, NY, USA, 10 pages. <https://doi.org/10.1145/3485447.3512199>

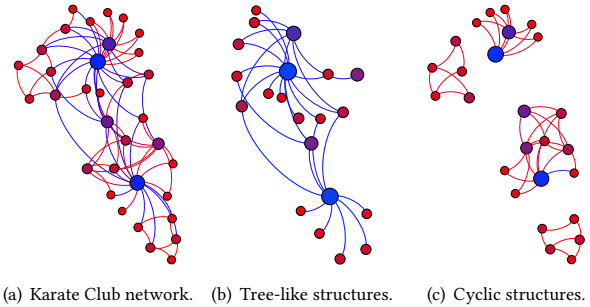
Permission to make digital or hard copies of all or part of this work for personal or classroom use is granted without fee provided that copies are not made or distributed for profit or commercial advantage and that copies bear this notice and the full citation on the first page. Copyrights for components of this work owned by others than ACM must be honored. Abstracting with credit is permitted. To copy otherwise, or republish, to post on servers or to redistribute to lists, requires prior specific permission and/or a fee. Request permissions from permissions@acm.org.

WWW '22, April 25–29, 2022, Virtual Event, Lyon, France

© 2022 Association for Computing Machinery.

ACM ISBN 978-1-4503-9096-5/22/04...\$15.00

<https://doi.org/10.1145/3485447.3512199>



(a) Karate Club network. (b) Tree-like structures. (c) Cyclic structures.

Figure 1: This is an example of a network of Karate Club [16]. We use Ricci curvature as edge weights to represent different local structures (tree-like and cyclic structures). It shows that one network contains heterogeneous topologies.

1 INTRODUCTION

Complex networks are widely used to model the complex relationships between objects [16, 64], such as social networks [20], academic networks [33, 52], and biological networks [15, 51]. In recent years, graph representation learning has shown its power in capturing the irregular but related complex structures in graph data [29, 31, 46]. The core assumption of graph representation learning is that topological properties are critical to representational capability [40, 41]. As the important topology characteristics, cycle and tree structures are ubiquitous in many real-world graphs, such as the cycle structure of family or friend relationships, the hypernym structure in natural languages [37, 53], the subordinate structure of entities in the knowledge graph [60], and the cascade structure of information propagation in social networks [69]. Since there are many unknowable noises in the real networks, these noises have huge impact on the topology of the network. Ignoring the existence of noise in the environment leads to the over-fitting problem in the learning process. In this paper, we focus on how to learn the generalization and robust representation for a graph.

Many generative adversarial networks (GAN) based methods [10, 25, 59, 67, 68] have been proposed to solve the above problem by using adversarial training regularization. However, there are two limitations of the existing GAN-based methods for robust representation of real-world graphs:

Discrete topology representation. Since the network is non-Euclidean geometry, the implementation of GAN-based methods on the network usually requires the topological-preserving constraints and performs the discrete operations in the network such as walking and sampling. Although these GAN-based methods can learn robust node representations, their generators focus on learning the

discrete node connection distribution in the original graph. The generated nodes do not accurately capture the graph topology and lead to serious distortion for graph representation. To address this issue, we aim to find a way to deal with the discrete topology of graphs as if it were continuous data. Fortunately, *Riemannian geometry* [62] provides a solid and manipulable mathematical framework. In recent works, certain types of graph data (e.g. hierarchical, scale-free, or cyclical graphs) have been shown to be better represented in non-Euclidean (Riemannian) geometries [7, 12, 13, 19, 37, 47–49]. Inspired by the unsupervised manifold hypothesis [8, 35, 42], we can understand a graph as a discretization of a latent geometric manifold¹. For example, the hyperbolic geometric spaces (with negative curvature) can be intuitively understood as a continuous tree [3, 24] and spherical geometry spaces (with positive curvature) benefit for modeling cyclical graphs [11, 12, 19, 65]. In these cases, the Riemannian geometric manifold has significant advantages by providing a better geometric prior and inductive bias for graphs with respective topological properties. Inspired by this property, we propose to learn robust graph representation in Riemannian geometric spaces.

Topological heterogeneity. There are some important properties (e.g., scale-free and small-world) usually presented by tree-like and cyclic structures [24, 39]. Meanwhile, these topological properties are also reflected in the density of the graph structure. As shown in Figure 1, the real-world graph data commonly has local structures with different topological properties, i.e., heterogeneous topologies. Moreover, the noisy edges [50] may seriously change the topological properties of local structures (e.g. a single binary tree structure with an extra edge may become a triangle). However, the Riemannian geometric manifold with constant curvature is regarded as global geometric priors of graph topologies, and it is difficult to capture the topological properties of local structures.

To address the above problems, we propose a novel **Curvature Graph Generative Adversarial Networks (CurvGAN)**. Specifically, we use a *constant curvature*² to measure the global geometric prior of the graph, and generalize GAN into the Riemannian geometric space with the constant curvature. As shown in Figure 2, an appropriate Riemannian geometric space ensures minimal topological distortion for graph embedding, leading to better and robust topology representation. For the discrete topology global representation, CurvGAN can directly perform any operations of GAN in the continuous Riemannian geometric space. For the topological heterogeneity issue, we design the *Ricci curvature regularization* to improve the local structures capture capability of the model. Overall, the contributions are summarized as follows:

- We propose a novel Curvature Graph Generative Adversarial Networks (CurvGAN), which is the first attempt to learn the robust node representations in a unified Riemannian geometric space.
- CurvGAN can directly generate fake neighbor nodes in continuous Riemannian geometric space conforming to the graph topological prior and better preserve the global and local topological properties by introducing various curvature metrics.

¹In this paper, the manifold is equivalent to embedding space, and we will use the terms *manifold* and *space* interchangeably.

²In this paper, the constant curvature of the graph is considered as the global average sectional curvature.

- Extensive experiments on synthetic and real-world datasets demonstrate a significant and consistent improvement in model robustness and efficiency with competitive performance.

2 PRELIMINARY

2.1 Riemannian Geometric Manifold

Riemannian geometry is a strong and elegant mathematical framework for solving non-Euclidean geometric problems in machine learning and manifold learning [7, 12, 27]. A manifold is a special kind of connectivity in which the coordinate transformation between any two (local) coordinate systems is continuous. *Riemannian manifold* [2] is a *smooth manifold* \mathcal{M} of dimension d with the *Riemannian metric* g , denoted as (\mathcal{M}, g) . At each point $\mathbf{x} \in \mathcal{M}$, the locally space looks like a d -dimension space, and it associates with the *tangent space* $\mathcal{T}_{\mathbf{x}}\mathcal{M}$ of d -dimension. For each point \mathbf{x} , the Riemannian metric g is given by an inner-product $g_{\mathbf{x}}(\cdot, \cdot) : \mathcal{T}_{\mathbf{x}}\mathcal{M} \times \mathcal{T}_{\mathbf{x}}\mathcal{M} \rightarrow \mathbb{R}$.

2.2 The κ -stereographic Model

The gyrovector space [54–57] formalism is used to generalize vector spaces to the Poincaré model of hyperbolic geometry [53]. The important quantities from Riemannian geometry can be rewritten in terms of the Möbius vector addition and scalar-vector multiplication [14]. However, these mathematical tools are used only in hyperbolic spaces (i.e., constant negative curvature). To extend these tools to unify all curvatures, [3] leverage gyrovector spaces to the κ -stereographic model.

Given a curvature $\kappa \in \mathbb{R}$, a n -dimension κ -stereographic model $(\text{st}_{\kappa}^d, g^{\kappa})$ can be defined by the manifold st_{κ}^d and Riemannian metric g^{κ} :

$$\text{st}_{\kappa}^d = \{\mathbf{x} \in \mathbb{R}^d \mid -\kappa \|\mathbf{x}\|_2^2 < 1\}, \quad (1)$$

$$g_{\mathbf{x}}^{\kappa} = \lambda_{\mathbf{x}}^{\kappa 2} g^{\mathbb{B}}, \text{ where } \lambda_{\mathbf{x}}^{\kappa} = 2/(1 + \kappa \|\mathbf{x}\|^2), \quad (2)$$

where $g^{\mathbb{B}} = \mathbf{I}^d$ is the Euclidean metric tensor. Note that when the curvature $\kappa > 0$, st_{κ}^d is \mathbb{R}^d , while for $\kappa < 0$, st_{κ}^d is a Poincaré ball of radius $1/\sqrt{-\kappa}$.

Distance. For any point pair $\mathbf{x}, \mathbf{y} \in \text{st}_{\kappa}^d$, $\mathbf{x} \neq \mathbf{y}$, the projection node $\mathbf{v} \neq 0$ the distance in κ -stereographic space is defined as:

$$d_{\text{st}}^{\kappa}(\mathbf{x}, \mathbf{y}) = (2/\sqrt{|\kappa|}) \tan_{\kappa}^{-1} \|\!-\mathbf{x} \oplus_{\kappa} \mathbf{y}\|. \quad (3)$$

Note that the distance is defined in all the cases except for $\mathbf{x} \neq -\mathbf{y}/\kappa \|\mathbf{y}\|^2$ if $\kappa > 0$.

Exponential and Logarithmic Maps. The manifold st_{κ}^d and the tangent space $\mathcal{T}_{\mathbf{x}}\text{st}_{\kappa}^d$ can be mapped to each other via *exponential map* and *logarithmic map*. The *exponential map* $\exp_{\mathbf{x}}^{\kappa}(\cdot)$ and *logarithmic map* $\log_{\mathbf{x}}^{\kappa}(\cdot)$ are defined as:

$$\exp_{\mathbf{x}}^{\kappa}(\mathbf{v}) := \mathbf{x} \oplus_{\kappa} \left(\tan_{\kappa} \left(\sqrt{|\kappa|} \frac{\lambda_{\mathbf{x}}^{\kappa} \|\mathbf{v}\|}{2} \right) \frac{\mathbf{v}}{\|\mathbf{v}\|} \right), \quad (4)$$

$$\log_{\mathbf{x}}^{\kappa}(\mathbf{y}) := \frac{2|\kappa|^{-\frac{1}{2}}}{\lambda_{\mathbf{x}}^{\kappa}} \tan_{\kappa}^{-1} \|\!-\mathbf{x} \oplus_{\kappa} \mathbf{y}\| \frac{-\mathbf{x} \oplus_{\kappa} \mathbf{y}}{\|\!-\mathbf{x} \oplus_{\kappa} \mathbf{y}\|}, \quad (5)$$

where $\tan_{\kappa} = \frac{1}{\sqrt{|\kappa|}} \tan(\cdot)$ and $\lambda_{\mathbf{x}}^{\kappa}$ is the conformal factor which comes from Riemannian metric.

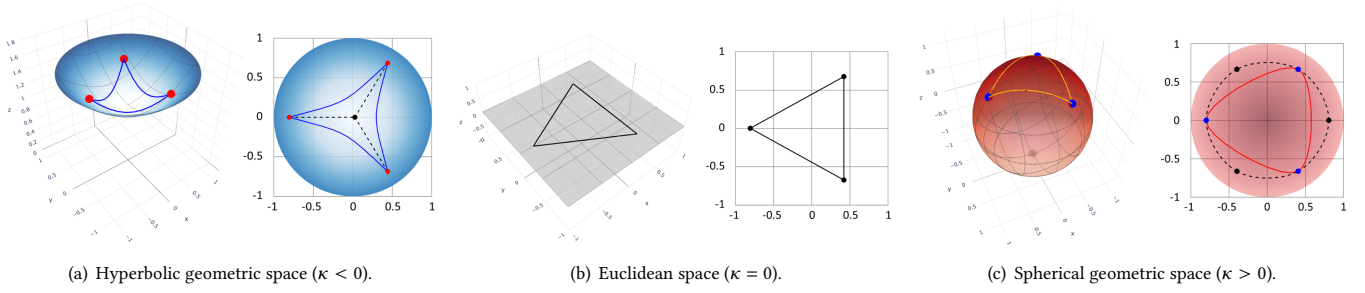


Figure 2: A toy example of a triangular structure in a Riemannian geometric space with different average sectional curvatures. (a) The geodesics (blue solid lines) of a triangular structure approximate a tree (dash lines and the virtual center) in hyperbolic geometric space. (b) A triangular structure in Euclidean space. (c) The triangular geodesics (red solid lines) approximate a cycle structure (dash lines and black virtual nodes) in spherical geometric space.

2.3 The Graph Curvature

Sectional Curvature. In Riemannian geometry, the sectional curvature [36] is one of the ways to describe the curvature of Riemannian manifolds. In existing works [3, 19, 45], average sectional curvature κ has been used as the constant curvature of non-Euclidean geometric embedding space.

Ricci Curvature. Ricci curvature [28, 36] is a broadly metric which measures the geometry of a given metric tensor that differs locally from that of ordinary Euclidean space. In machine learning, Ricci curvature is transformed into edge weights to measure local structural properties [66]. Ollivier-Ricci curvature [38] is a coarse approach used to compute the Ricci curvature for discrete graphs.

3 CURVGAN MODEL

In this section, we present a novel Curvature Graph Generative Adversarial Network (CurvGAN) in the latent geometric space of the graph. The overall architecture is shown in Figure 3.

3.1 Geometric Prior of Graph Topology

An interesting theory of graph geometry is that some typical topological structures can be described intuitively using Riemannian geometry with different curvature κ [5], i.e., hyperbolic ($\kappa < 0$), Euclidean ($\kappa = 0$) and spherical ($\kappa > 0$) geometries. As shown in Figure 2, the hyperbolic space can be intuitively understood as a continuous tree [24], and spherical geometry provides benefits for learning cyclical structure [11, 18, 19, 63, 65]. Therefore, we can learn better graph representation with minimal embedding distortion in an appropriate Riemannian geometric space [3]. Motivated by this idea, we first search for an appropriate Riemannian geometric space to approximate the global topological properties of the graph, and then we capture the local structural features for each node by introducing Ricci curvature. In this way, we propose a curvature-constrained framework to capture both the global topology and local structure of the graph.

Global Curvature Estimation. In machine learning, the Riemannian manifold is commonly considered as a geometric prior with constant curvature. For a graph embedding in Riemannian geometric space, a key parameter is *constant curvature* κ , which can affect the embedding distortion of a graph topology [19]. To

minimize the embedding distortion and explore the optimal curvature, we leverage the average sectional curvature estimation algorithm [3, 19] to estimate global curvature. Specifically, let (a, b, c) be a geodesic triangle in manifold st_κ^d , and m be the (geodesic) midpoint of (b, c) . Their quantities are defined as follows:

$$\xi_{\text{st}}(a, b, c) = p_{\text{st}}(a, m)^2 + \frac{p_{\text{st}}(b, c)^2}{4} + \frac{p_{\text{st}}(a, b)^2 + p_{\text{st}}(a, c)^2}{2}, \quad (6)$$

$$\xi_{\text{st}}(m; a, b, c) = \frac{1}{2p_{\text{st}}(a, m)} \xi_{\text{st}}(a, b, c).$$

We design our curvature updating according to Eq. (6). The new average curvature estimation κ is defined as:

$$\kappa = \frac{1}{|V|} \sum_{m \in V} \left(\frac{1}{n_s} \sum_{j=0}^{n_s} \xi_{\text{st}}(\mathbf{h}_m; \mathbf{h}_{a_j}, \mathbf{h}_{b_j}, \mathbf{h}_{c_j}) \right), \quad (7)$$

where b and c are randomly sampled from the neighbors of m , and a is a node in the graph G except for $\{m, b, c\}$. For each node, we sample n_s times and take the average as the estimated curvature.

Local Curvature Computation. To deal with the embedding distortion caused by topological heterogeneity, we also need to consider the local structural properties of the graph. We leverage the *Ollivier-Ricci curvature* [38] to solve this problem. Specifically, Ollivier-Ricci curvature $\kappa_r(x, y)$ of the edge (x, y) is defined as:

$$\kappa_r(x, y) = \frac{W(m_x, m_y)}{d(x, y)}, \quad (8)$$

where $W(\cdot, \cdot)$ is the Wasserstein distance, $d(\cdot, \cdot)$ is the geodesic distance (embedding distance), and m_x is the mass distribution of node x . The mass distribution represents the importance distribution of a node and its one-hop neighborhood [38], which is defined as:

$$m_x^\alpha = \begin{cases} \alpha & \text{if } x_i = x, \\ 1 - \alpha & \text{if } x_i \in \text{Neighbor}(x), \\ 0 & \text{otherwise,} \end{cases} \quad (9)$$

where α is a hyper-parameter that represents the importance of node x and we take $\alpha = 0.5$ following the existing works [44, 66].

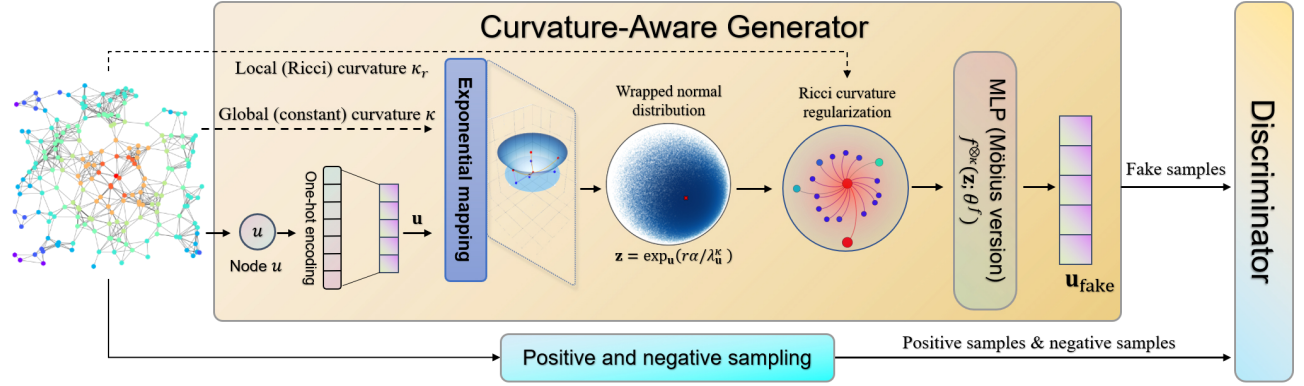


Figure 3: An illustration of CurvGAN architecture. (1) CurvGAN estimates the constant curvature κ and Ricci curvature κ_r of the graph; (2) CurvGAN’s generator generates negative samples by sampling fake node representations from the wrapper normal distribution; (3) CurvGAN’s discriminator discriminates the positive, negative and generated fake samples.

3.2 Curvature-Aware Generator

Curvature-Aware Generator aims to directly generate fake nodes from the continuous Riemannian geometric space of the global topology as the enhanced negative samples while preserving the local structure information of the graph as much as possible.

Global Topological Representation Generation. First, we map a node u into the Riemannian geometric space with the global curvature κ , and input it to an embedding layer of Möbius version to get a dense vector representation. In order to generate appropriate representations of fake neighbor nodes, we need to extend the noise distribution to the Riemannian geometric space. An approach is to use exponential mapping to map a normal distribution into a Riemannian manifold, and this distribution measure is referred to as the *wrapped normal distribution* [17, 34]. The d -dimensional wrapped normal distribution $\mathcal{N}_{\text{st}}^\kappa(\mathbf{z}|\boldsymbol{\mu}, \sigma^2\mathbf{I})$ is defined as:

$$\begin{aligned} \mathcal{N}_{\text{st}}^\kappa(\mathbf{z}|\boldsymbol{\mu}, \sigma^2\mathbf{I}) & \\ &= \mathcal{N}\left(\lambda_\mu^\kappa \log_\mu(\mathbf{z}) \mid \mathbf{0}, \sigma^2\mathbf{I}\right) \left(\frac{\sqrt{\kappa} d_{\text{st}}^\kappa(\boldsymbol{\mu}, \mathbf{z})}{\sinh(\sqrt{\kappa} d_{\text{st}}^\kappa(\boldsymbol{\mu}, \mathbf{z}))} \right)^{d-1}, \end{aligned} \quad (10)$$

where $\boldsymbol{\mu} \in \text{st}_\kappa^d$ is the mean parameter, and $\sigma \in \mathbb{R}^d$ is the variance. Then we can introduce a reparameterized sampling strategy to generate the negative node representation. Specifically, for a fake node \mathbf{u}_{fake} in the manifold st , we can generate the noisy representation in the Riemannian geometric space, given by

$$\mathbf{z}_{\mathbf{u}_{\text{fake}}}^\mathcal{G} = \exp_{\mathbf{u}}^\kappa\left(\frac{r}{\lambda_{\mathbf{u}}^\kappa}\boldsymbol{\alpha}\right), \text{ with } \mathbf{u}_{\text{fake}} \sim \mathcal{N}(0, \sigma^2\mathbf{I}), \quad (11)$$

with radius $r = d_{\text{st}}^\kappa$, direction $\boldsymbol{\alpha} = \frac{\mathbf{v}}{r}$, and $\mathbf{u} \in \text{st}_\kappa^d$ is the embedding vector of node u .

Local Structure Preserving Regularization. Since the real-world graph data usually has a heterogeneous topology, the edge generated by data noise may seriously change the local structure, leading to the following two issues: (1) the model cannot capture the correct local structure, leading to the generated sample may have different properties from the original structure: (2) the fake samples generated by the model are no longer indistinguishable from the real

samples. Therefore, we need to regularize the generated fake nodes by using a measurement of preserving local structure information. If two nodes are similar in the same local structure, they should have the same Ricci curvatures in the neighborhood.

According to Eq. (8), the regularization term can be given by

$$\text{Reg}(\kappa_r^u, \kappa_r^{\mathbf{u}_{\text{fake}}}) = \frac{1}{|\mathbb{N}(u)|} \sum_{v \in \mathbb{N}(u)} \left(1 - \frac{W(m_u, m_v)d(u_{\text{fake}}, v)}{W(m_{\mathbf{u}_{\text{fake}}}, m_v)d(u, v)} \right), \quad (12)$$

where $\mathbb{N}(u)$ is the neighbors of node u . To facilitate the calculation of Ricci curvature [38], we assume the generated fake node has a similar one-hop neighborhood as the original node u , i.e., $m_u = m_{\mathbf{u}_{\text{fake}}}$.

Fake Sample Generation Strategy. Given a node u , the generator outputs the embedding $\mathbf{z}_{\mathbf{u}_{\text{fake}}}^\mathcal{G} = G_{\text{st}}^\kappa(\mathbf{u}; \theta_{\text{st}}^\kappa)$ of the fake node \mathbf{u}_{fake} as a substitute for node u . In this way, we can obtain a node-pair set $\{(v, \mathbf{u}_{\text{fake}}), v \in \mathbb{N}(u)\}$ as the negative samples. The generator of Riemannian latent geometry is defined as:

$$\begin{aligned} G_{\text{st}}^\kappa(\cdot; \theta_{\text{st}}^\kappa) &= f^{\otimes \kappa}(\mathbf{z}; \theta^f), \\ f^{\otimes \kappa} &= \exp_{\mathbf{u}}^\kappa(f(\log_{\mathbf{u}}^\kappa(\mathbf{u}))), \end{aligned} \quad (13)$$

where $\theta_{\text{st}}^\kappa$ is the parameters for generator G_{st}^κ , and $f^{\otimes \kappa}$ is a Möbius version of the multi-layer perception.

Optimization of Generator. For the high-order proximity of each node-pair in a graph, the advantage of our CurvGAN is that it doesn’t require traversing the shortest path between two points to compute the connectivity probability. According to Eq. (12), when the embedding distortion is minimal, the longer the shortest path between any two nodes, the less probability of this node-pair by direct calculation in the latent geometric space, and vice versa. The loss function of the generator is defined as follows:

$$\begin{aligned} \mathcal{L}_G &= \mathbb{E}_{u \in \mathcal{V}} \log \left(1 - D^\kappa(\mathbf{u}^D, \mathbf{u}_{\text{fake}}) \right) \\ &+ \lambda \left\| \sum_{u \in \mathcal{V}} \text{Reg}(\kappa_r^u, \kappa_r^{\mathbf{u}_{\text{fake}}}) \right\|_2. \end{aligned} \quad (14)$$

3.3 Discriminator

The discriminator of CurvGAN aims to determine whether the connection between two nodes is real. For node pair (u, v) , the discriminant function outputs the connection probability between two nodes. In general, the discriminator D is defined as:

$$D^\kappa(u, v; \theta^D) = \mathcal{F}_\kappa(u, v; \theta^F), \quad (15)$$

where θ^D is the parameters of discriminator D .

For *link prediction* task, we use the Fermi-Dirac decoder [24, 37] to compute the connection probability:

$$\mathcal{F}_\kappa(u, v; \theta^F) = \left[e^{(\mathbf{d}_{\text{st}}^\kappa(u, v)^2 - \rho) / \tau} + 1 \right]^{-1}, \quad (16)$$

where $\mathbf{d}_{\text{st}}^\kappa$ is the hyperbolic distance in Eq. (3) and (ρ, τ) are hyper-parameters of Fermi-Dirac distribution.

For *node classification* task, inspired by [9], we map the output embedding $\mathbf{z}_i, i \in \mathcal{V}$ to the tangent space \mathcal{T}_{ost} by logarithmic mapping $\log_{\text{o}}^\kappa(\mathbf{z}_i)$, then perform Euclidean multinomial logistic regression, where o is the north pole or origin.

For a graph $\mathcal{G}(\mathcal{V}, \mathcal{E})$, the input samples of the discriminator are as follows:

- Positive Sample (u, v) : There indeed exists a directed edge from u to v on a graph \mathcal{G} .
- Negative Samples (u, w) and (u_{fake}, v) : For a given node $u, w, v \in \mathcal{V}$, the negative samples consists of the samples by negative sampling in the original graph $(u, w) \notin \mathcal{E}$ and the fake samples (u_{fake}, v) generated by the generator.

Optimization of Discriminator. The loss function of positive samples (u, v) is:

$$\mathcal{L}_{\text{pos}}^D = \mathbb{E}_{(u, v) \sim \mathcal{E}} - \log D^\kappa(\mathbf{u}^D, \mathbf{u}_{\text{pos}}^D). \quad (17)$$

The loss function of negative samples (u, w) and (u_{fake}, v) is defined as:

$$\begin{aligned} \mathcal{L}_{\text{neg}}^D = & \mathbb{E}_{u \in \mathcal{V}} - (\log(1 - D^\kappa(\mathbf{u}^D, \mathbf{u}_{\text{neg}}^D)) \\ & + \log(1 - D^\kappa(\mathbf{u}^D, \mathbf{u}_{\text{fake}}^D))). \end{aligned} \quad (18)$$

Then we integrate the above Eq. (17) and Eq. (18) as the loss function of the discriminator, which we try to minimize:

$$\mathcal{L}^D = \mathcal{L}_{\text{pos}}^D + \mathcal{L}_{\text{neg}}^D. \quad (19)$$

3.4 Training and Complexity Analysis

The overall training algorithm for CurvGAN is summarized in Algorithm 1. For each training epoch, time complexity of CurvGAN per epoch is $O(n_s \cdot (n_e^D \cdot |\mathcal{E}| + n_e^G \cdot (|\mathcal{V}| + n_s \log(n_s))) \cdot d^2)$. Since n_s, n_e^G, n_e^D and d are small constants, CurvGAN's time complexity is linear to $|\mathcal{V}|$ and $|\mathcal{E}|$. The space complexity of CurvGAN is $O(2 \cdot d \cdot (|\mathcal{V}| + |\mathcal{E}|))$. In conclusion, CurvGAN is both time and space-efficient, making it scalable for large-scale graphs.

4 EXPERIMENT

In this section, we conduct comprehensive experiments to demonstrate the effectiveness and adaptability of CurvGAN³ on various datasets and tasks. We further analyze the robustness to investigate the expressiveness of CurvGAN.

³Code is available at <https://github.com/RingBDStack/CurvGAN>.

Algorithm 1: CurvGAN

Input: Graph $\mathcal{G} = \{V, E\}$; Number of training epochs n_e , generator's epochs n_e^G , discriminator's epochs n_e^D ; Number of samples n_s .

Output: Predicted result of the downstream task.

// Curvature Estimation

- 1 $\kappa \leftarrow$ Eq. (7);
- 2 $\kappa_r \leftarrow$ Eq. (8);
- 3 **for** $t = 1, 2, \dots, n_e$ **do**
- // Train Discriminator
- 4 **for** $d = 1, 2, \dots, n_e^D$ **do**
- // Sample neighbour $v \in \mathcal{N}(u)$ for each $u \in V$
- $\mathbf{u}_{\text{pos}} \leftarrow$ RANDOMWALK(u, n_s);
- // Sample negative nodes and generate fake nodes
- $\mathbf{u}_{\text{neg}} \leftarrow$ RANDOMSELECT(V, n_s);
- $\mathbf{u}_{\text{fake}} \leftarrow$ Eq. (13);
- // Optimize
- $\mathcal{L}_D \leftarrow$ Eq. (14);
- 9 **end**
- // Train Generator
- 10 **for** $g = 1, 2, \dots, n_e^G$ **do**
- // Generate fake nodes
- $\mathbf{u}_{\text{fake}} \leftarrow$ Eq. (13);
- $\text{Reg}(\kappa_r^{\text{fake}}, \kappa_r^{\text{true}}) \leftarrow$ Eq. (12);
- // Optimize
- $\mathcal{L}_G \leftarrow$ Eq. (19);
- 14 **end**
- 15 **end**

Table 1: Statistics of datasets.

	Dataset	#Nodes	#Edges	Avg. Degree	#Labels	κ
Synth.	SBM	1,000	15,691	15.69	5	-1.496
	BA	1,000	2,991	2.99	5	-1.338
	WS	1,000	11,000	11.00	5	0.872
Real	Cora	2,708	5,429	3.90	7	-2.817
	Citeseer	3,312	4,732	2.79	6	-4.364
	Polblogs	1,490	19,025	25.54	2	-0.823

4.1 Datasets.

We conduct experiments on synthetic and real-world datasets to evaluate our method, and analyze model's capabilities in terms of both graph theory and real-world scenarios. The statistics of datasets are summarized in Table 1.

Synthetic Datasets. We generate three synthetic graph datasets using several well-accepted graph theoretical models: **Stochastic Block Model (SBM)** [21], **Barabási-Albert (BA)** scale-free graph model [4], and **Watts-Strogatz (WS)** small-world graph model [61]. For each dataset, we create 1,000 nodes and subsequently perform the graph generation algorithm on these nodes. For the SBM graph,

Table 2: Summary of link prediction AUC scores (%), node classification Micro-F1 and Macro-F1 scores (%) on synthetic graphs. (Result: average score \pm standard deviation; Bold: best; Underline: runner-up.)

Method	Stochastic Block Model			Barabási-Albert			Watts-Strogatz			Avg.Rank
	AUC	Micro-F1	Macro-F1	AUC	Micro-F1	Macro-F1	AUC	Micro-F1	Macro-F1	
GAE [22]	50.13 \pm 0.12	24.07 \pm 1.12	21.94 \pm 2.11	50.26 \pm 0.21	39.35 \pm 1.72	17.83 \pm 1.11	50.10 \pm 0.08	19.08 \pm 1.87	16.47 \pm 2.64	6.6
VGAE [22]	50.32 \pm 1.49	20.47 \pm 2.05	15.41 \pm 1.11	62.43 \pm 1.26	37.44 \pm 1.73	15.88 \pm 2.31	49.94 \pm 0.57	19.14 \pm 1.40	12.02 \pm 1.13	7.2
DGI [58]	49.88 \pm 0.51	19.06 \pm 1.87	12.13 \pm 2.08	70.90 \pm 2.12	38.24 \pm 1.11	18.13 \pm 0.26	49.55 \pm 0.49	18.27 \pm 1.14	13.31 \pm 0.80	8.1
G2G [6]	79.45 \pm 1.28	21.44 \pm 0.05	20.98 \pm 0.03	54.29 \pm 1.62	42.27 \pm 0.31	23.96 \pm 0.39	<u>73.15\pm2.23</u>	22.89 \pm 0.07	22.75 \pm 0.07	5.1
GraphGAN [59]	84.56 \pm 2.84	38.60 \pm 0.51	38.87 \pm 0.32	63.34 \pm 4.19	43.60 \pm 0.61	<u>24.57\pm0.53</u>	66.63 \pm 9.46	<u>41.80\pm0.84</u>	41.76\pm1.25	<u>3.0</u>
ANE [10]	85.09 \pm 1.12	39.88 \pm 1.06	33.85 \pm 1.75	62.13 \pm 2.49	<u>46.04\pm3.01</u>	19.32 \pm 2.66	62.98 \pm 1.44	33.84 \pm 2.75	33.51 \pm 2.00	3.7
\mathcal{P} -VAE [32]	<u>86.10\pm0.97</u>	<u>57.94\pm1.29</u>	<u>52.97\pm1.47</u>	<u>76.08\pm1.22</u>	38.38 \pm 1.37	20.03 \pm 0.32	51.43 \pm 3.56	19.85 \pm 1.40	13.62 \pm 1.62	4.7
Hype-ANE [30]	82.29 \pm 2.70	18.84 \pm 0.32	11.93 \pm 0.09	70.92 \pm 0.43	56.92\pm2.41	31.58\pm1.17	63.34 \pm 4.19	33.40 \pm 2.55	32.94 \pm 2.70	4.4
CurvGAN (Ours)	89.74\pm0.70	59.00\pm0.56	55.99\pm2.20	95.87\pm0.86	42.50 \pm 1.37	19.28 \pm 0.64	88.67\pm0.22	43.10\pm1.78	<u>35.21\pm1.95</u>	1.8

Table 3: Summary of link prediction AUC scores (%), node classification Micro-F1 and Macro-F1 scores (%) on real-world graphs. (Result: average score \pm standard deviation; Bold: best; Underline: runner-up.)

Method	Cora			Citeseer			Polblogs			Avg.Rank
	AUC	Micro-F1	Macro-F1	AUC	Micro-F1	Macro-F1	AUC	Micro-F1	Macro-F1	
GAE [22]	86.12 \pm 0.87	80.92 \pm 0.99	79.55 \pm 1.32	87.25 \pm 1.26	58.50 \pm 3.31	50.41 \pm 3.32	83.55 \pm 0.62	89.50 \pm 0.53	89.42 \pm 0.53	4.4
VGAE [22]	85.94 \pm 0.05	79.95 \pm 0.95	78.79 \pm 0.97	85.72 \pm 2.20	63.75 \pm 1.39	55.47 \pm 1.34	88.12 \pm 0.64	87.02 \pm 1.04	86.98 \pm 0.88	5.8
DGI [58]	75.39 \pm 0.29	74.09 \pm 1.75	66.70 \pm 1.91	81.30 \pm 3.57	73.16\pm0.68	<u>63.27\pm0.63</u>	76.33 \pm 3.35	87.11 \pm 1.18	87.06 \pm 1.19	6.3
G2G [6]	84.47 \pm 0.70	82.13 \pm 0.58	81.14 \pm 0.40	<u>90.34\pm1.44</u>	<u>71.03\pm0.27</u>	66.44\pm0.32	<u>91.02\pm0.29</u>	87.52 \pm 0.28	87.51 \pm 0.28	<u>3.3</u>
GraphGAN [59]	82.50 \pm 0.64	76.40 \pm 0.21	76.80 \pm 0.34	74.50 \pm 0.02	49.80 \pm 1.02	45.70 \pm 0.13	69.80 \pm 0.26	77.45 \pm 0.64	76.90 \pm 0.43	8.4
ANE [10]	83.10 \pm 0.57	<u>83.00\pm0.51</u>	<u>81.90\pm1.40</u>	83.00 \pm 1.20	50.20 \pm 0.12	49.50 \pm 0.61	73.09 \pm 0.76	<u>95.07\pm0.65</u>	<u>95.06\pm0.65</u>	4.8
\mathcal{P} -VAE [32]	<u>86.72\pm0.67</u>	79.57 \pm 2.16	77.50 \pm 2.46	88.69 \pm 1.00	67.91 \pm 1.65	60.20 \pm 1.93	85.40 \pm 2.23	87.74 \pm 1.28	87.68 \pm 1.26	4.2
Hype-ANE [30]	74.50 \pm 0.53	80.70 \pm 0.07	79.20 \pm 0.28	85.80 \pm 0.53	64.40 \pm 0.29	58.70 \pm 0.02	64.27 \pm 0.73	95.62\pm0.35	95.61\pm0.36	5.0
CurvGAN (Ours)	94.00\pm0.63	84.50\pm0.53	85.60\pm0.25	93.80\pm0.15	65.60 \pm 0.27	59.60 \pm 0.21	93.88\pm0.42	88.89 \pm 0.17	87.65 \pm 0.25	2.4

we equally partition all nodes into 5 communities with the intra-class and inter-class probabilities $(p, q) = (0.21, 0.025)$. For the Barabási-Albert graph, we set the number of edges from a new node to existing nodes to a random number between 1 and 10. For the Watts-Strogatz graph, each node is connected to 24 nearest neighbors in the cyclic structure, and the probability of rewiring each edge is set to 0.21. For each generated graph, we randomly remove 50% nodes as the test set with other 50% nodes as the positive samples and generate or sample the same number of negative samples.

Real-world Datasets. We also conducted experiments on three real-world datasets: **Cora** [43] and **Citeseer** [23] are citation networks of academic papers; **Polblogs** [1] is political blogs in 2004 U.S. president election where nodes are political blogs and edges are citations between blogs. The training settings for the real-world datasets are the same as settings for synthetic datasets.

4.2 Experimental Setup

Baselines. To evaluate the proposed CurvGAN, we compare it with a variety of baseline methods including: (1) **Euclidean graph representation methods:** We compare with other state-of-the-art unsupervised graph learning methods. GAE [22] and VGAE [22] are the autoencoders and variational autoencoder for graph representation learning; G2G [6] embeds each node of the graph as a Gaussian distribution and captures uncertainty about the node representation; DGI [58] is an unsupervised graph contrastive learning model

by maximizing mutual information. (2) **Euclidean graph generative adversarial networks:** GraphGAN [59] learns the sampling distribution to sample negative nodes from the graph; ANE [10] trains a discriminator to push the embedding distribution to match the fixed prior; (3) **Hyperbolic graph representation learning:** \mathcal{P} -VAE [32] is a variational autoencoder by using Poincaré ball model in hyperbolic geometric space; Hyper-ANE [30] is a hyperbolic adversarial network embedding model by extending ANE to hyperbolic geometric space.

Settings. The parameters of baselines are set to the default values in the original papers. For CurvGAN, we choose the numbers of generator and discriminator training iterations per epoch $n_e^G = 10$, $n_e^D = 10$. The node embedding dimension of all methods is set to 16. The reported results are the average scores and standard deviations over 5 runs. All models were trained and tested on a single Nvidia V100 32GB GPU.

4.3 Synthetic Graph Datasets

To verify the topology-preserving capability, we evaluate our method on synthetic graphs generated by the well-accepted graph theoretical models: **SBM**, **BA**, and **WS** graphs. These three synthetic graphs can represent three typical topological properties: the SBM graph has more community-structure, the BA scale-free graph has more tree-like structure, and the WS small-world graph has more cyclic structure. We evaluate the performance, generalization and robustness of our method comprehensively on these graphs with different topological properties.

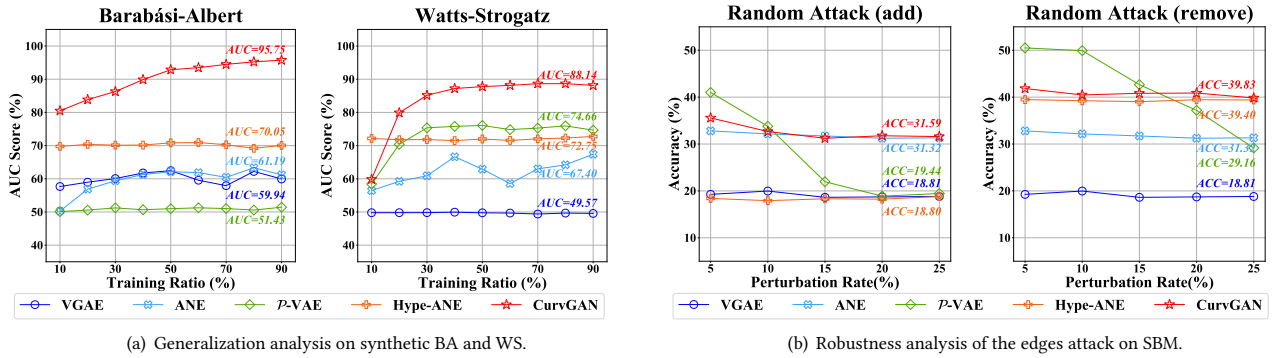


Figure 4: Generalization and robustness analysis on synthetic data.

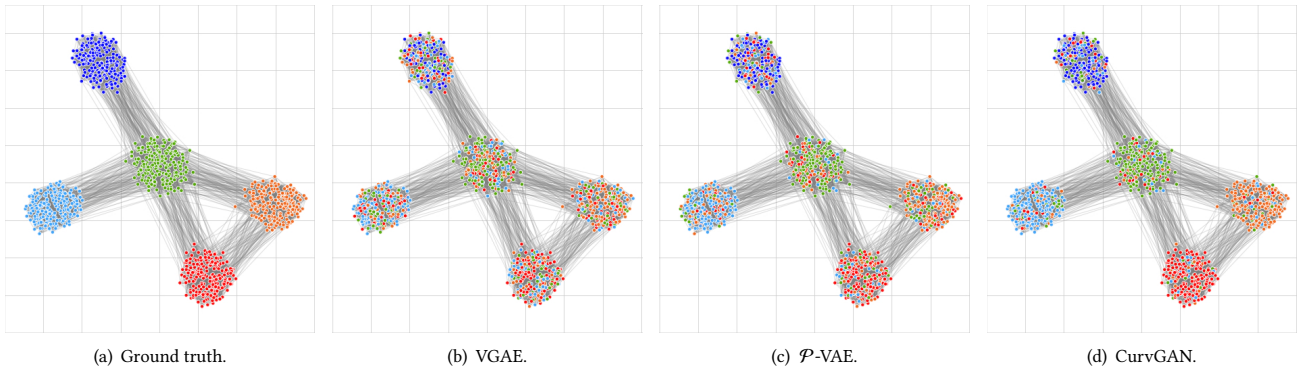


Figure 5: Visualization of classification results for random attack of 10% extra edges on SBM graph.

Performance on Benchmarks. Table 2 summarizes the performance of CurvGAN and all baselines on the synthetic datasets. For the link prediction task, the performance of a model indicates the capture capability of topological properties. It can be observed that the hyperbolic geometric model performs better in SBM and BA graphs than in WS graphs. The reason is that SBM and BA graphs are more "tree-like" than the WS graph. Our CurvGAN outperforms all baselines in three synthetic graphs. The result shows that a good geometry prior is very important for the topology-preserving. CurvGAN can adaptively select hyperbolic or spherical geometric space by estimating the optimal geometric prior. For the node classification task, the GAN-based methods generally outperform other methods because the synthetic graphs only have topological structure and no node features. The GAN-based method can generate more samples to help the model fit the data distribution. The results show that our CurvGAN also has the best comprehensive competitiveness in node classification benefit from the stronger negative samples.

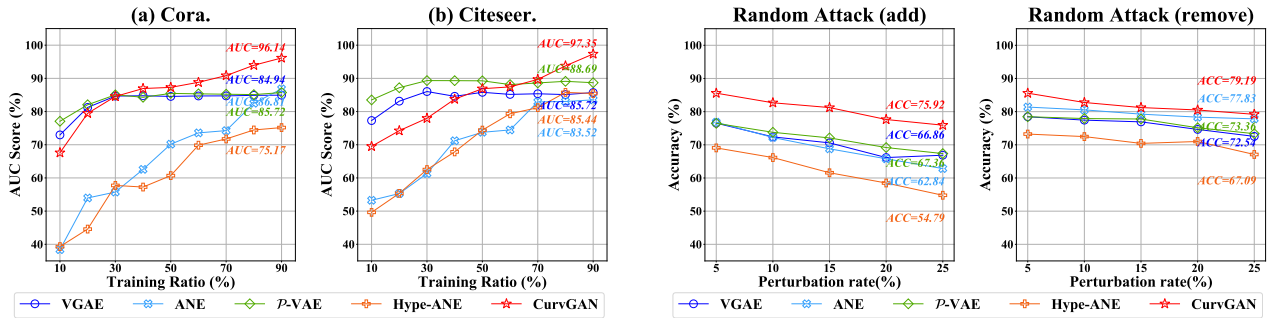
Generalization Analysis. We evaluate the generalization capability of the model by setting different proportions of the training set. Figure 4 (a) shows the performances of link prediction with different training ratios. CurvGAN significantly outperforms all baselines, even when the training ratio is small. In addition, CurvGAN gains more stable performances than other GAN-based methods across all datasets, which demonstrates the excellent structure-preserving capability of the network latent geometric space. We observe an interesting phenomenon: the non-Euclidean geometry models have very smooth performances on the synthetic graphs with a single

topological property. It demonstrates again that a single negative curvature geometry lacks generalization capability for different graph datasets.

Robustness Analysis. Considering a poisoning attack scenario, we leverage the RAND attack, provided by DeepRobust [26] library, to randomly add or remove fake edges into the graph. Specifically, we randomly remove and add edges of different ratios (from 5% to 25%) as the training data respectively, and randomly sample 10% nodes edges from the original network as the test data. The results are shown in Figure 4 (b). CurvGAN consistently outperforms Euclidean and hyperbolic models in different perturbation rates. Figure 5 shows the visualization of an edge attack scenario. It can be observed that P-VAE has no significant improvement than Euclidean VGAE. Since noisy edges may perturb some tree-like structures of the original SBM graph, leading to hyperbolic models no longer suitable for the perturbed graph topology. Overall, our CurvGAN has significant advantages in terms of robustness.

4.4 Real-world Graph Datasets

To verify the practicality of our model, we evaluate CurvGAN in terms of performance, generalization, and robustness on real-world datasets for two downstream tasks: link prediction and node classification. As in Section 4.3, we use the same unsupervised training setup on three real-world datasets, **Cora**, **Citseer**, and **Polblogs**. In addition, we also analyze the computational efficiency of CurvGAN and all baselines.



(a) Generalization analysis on Cora and Citeseer.

(b) Robustness analysis of the edges attack on Cora.

Figure 6: Generalization and robustness analysis on real-world data.

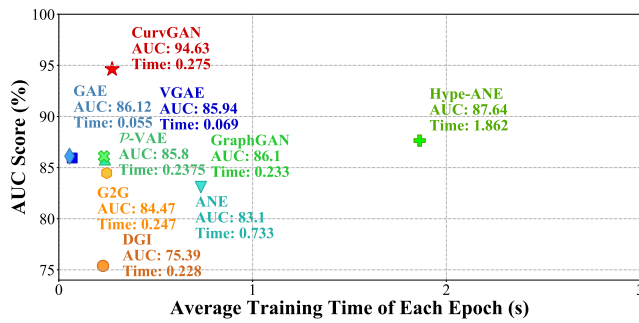


Figure 7: Training efficiency analysis.

Performance on Benchmarks. Table 3 summarizes the performance of CurvGAN and all baselines on three real-world datasets. For the link prediction task, our CurvGAN outperforms all baselines (including hyperbolic geometry models) in real data and can learn better structural properties based on correct topological geometry priors. In contrast to a single hyperbolic geometric space, a unified latent geometric space can improve benefits for learning better graph representation in real-world datasets with complex topologies. For the node classification task, we combine the above link prediction objective as the regularization term in node classification tasks, to encourage embeddings preserving the network structure. Table 3 also summarizes Micro-F1 and Macro-F1 scores of all models on three real-world datasets. It can be observed that the Euclidean models have comparative performance. The reason is that the node labels are more dependent on other features (e.g. node’s attributes or other information) than topological features.

Generalization Analysis. Figure 6 (a) shows the performances of link prediction with different training ratios. CurvGAN significantly outperforms all baselines even when the training ratio is small. In addition, we find that the stability of the autoencoders VGAE and P-VAE is higher than the GAN-based methods (ANE, GraphGAN, Hype-ANE and our CurvGAN), although their performances are outperformed by CurvGAN rapidly. The reason is the GAN-based method needs more samples to fit the data distribution.

Robustness Analysis. To evaluate the robustness of the model, we also perform a poisoning attack RAND by DeepRobust [26] on

the real-world data, and the setting is the same as in the robustness analysis in Section 4.3. Figure 6 (b) shows that CurvGAN and all baselines under the edges attack scenario on Cora. Our CurvGAN always has better performance even when the network is very noisy. Riemannian geometry implies the prior information of the network, making CurvGAN has the excellent denoising capability.

Efficiency Analysis. Figure 7 illustrates the training time of CurvGAN and baselines on Cora for link prediction. CurvGAN has both the best performance and second-best efficiency. It can be observed that our CurvGAN has the best computational efficiency in the GAN-based method (ANE, GraphGAN, and Hype-ANE). In general, the results show that the comprehensive evaluation of our model outperforms baselines on all datasets, which indicates that the network latent geometry can significantly improve the computational efficiency and scalability of network embedding.

5 CONCLUSION

In this paper, we proposed CurvGAN, a novel curvature graph generative adversarial network in Riemannian geometric space. CurvGAN is the first attempt to combine the generative adversarial network and Riemannian geometry, to solve the problems of network discrete topology representation and topological heterogeneity. For graphs with different topological properties, CurvGAN can effectively estimate a constant curvature to select an appropriate Riemannian geometry space, and leverage Ricci curvature regularization for capturing local structure. Moreover, CurvGAN’s generator and discriminator can perform operations and continuous computation for any node-pairs in the latent geometric space, leading to good efficiency and scalability. The experimental results on synthetic and real-world datasets demonstrate that CurvGAN consistently and significantly outperforms various state-of-the-arts unsupervised methods in terms of performance, generalization, and robustness.

ACKNOWLEDGMENTS

The authors of this paper were supported by the NSFC through grants (No.U20B2053), and the ARC DECRA Project (No.DE200100964). The corresponding author is Jianxin Li.

REFERENCES

- [1] Lada A Adamic and Natalie Glance. 2005. The political blogosphere and the 2004 US election: divided they blog. In *LinkKDD*. 36–43.
- [2] Stephanie Alexander. 1978. Michael Spivak, A comprehensive introduction to differential geometry. *Bull. Amer. Math. Soc.* 84, 1 (1978), 27–32.
- [3] Gregor Bachmann, Gary Bécigneul, and Octavian Ganea. 2020. Constant curvature graph convolutional networks. In *ICML*. PMLR, 486–496.
- [4] Albert-László Barabási and Réka Albert. 1999. Emergence of scaling in random networks. *Science* 286, 5439 (1999), 509–512.
- [5] Marian Boguna, Ivan Bonamassa, Manlio De Domenico, Shlomo Havlin, Dmitri Krioukov, and M Ángeles Serrano. 2021. Network geometry. *Nature Reviews Physics* 3, 2 (2021), 114–135.
- [6] Aleksandar Bojchevski and Stephan Günnemann. 2018. Deep Gaussian Embedding of Graphs: Unsupervised Inductive Learning via Ranking. In *ICLR*.
- [7] Michael M Bronstein, Joan Bruna, Yann LeCun, Arthur Szlam, and Pierre Vandergheynst. 2017. Geometric deep learning: going beyond euclidean data. *IEEE Signal Processing Magazine* 34, 4 (2017), 18–42.
- [8] Lawrence Cayton. 2005. Algorithms for manifold learning. *Univ. of California at San Diego Tech. Rep* 12, 1-17 (2005), 1.
- [9] Ines Chami, Zhitao Ying, Christopher Ré, and Jure Leskovec. 2019. Hyperbolic Graph Convolutional Neural Networks. In *NeurIPS*. 4869–4880.
- [10] Quanyu Dai, Qiang Li, Jian Tang, and Dan Wang. 2018. Adversarial network embedding. In *AAAI*. 2167–2174.
- [11] Tim R Davidson, Luca Falorsi, Nicola De Cao, Thomas Kipf, and Jakub M Tomczak. 2018. Hyperspherical variational auto-encoders. *UAI* (2018).
- [12] Michaël Defferrard, Nathanaël Perraudin, Tomasz Kacprzak, and Raphael Sgier. 2019. DeepSphere: towards an equivariant graph-based spherical cnn. *ICLR* (2019).
- [13] Xingcheng Fu, Jianxin Li, Jia Wu, Qingyun Sun, Cheng Ji, Senzhang Wang, Jiajun Tan, Hao Peng, and S Yu Philip. 2021. ACE-HGNN: Adaptive Curvature Exploration Hyperbolic Graph Neural Network. In *ICDM*. IEEE, 111–120.
- [14] Octavian-Eugen Ganea, Gary Bécigneul, and Thomas Hofmann. 2018. Hyperbolic Neural Networks. In *NeurIPS*, Samy Bengio, Hanna M. Wallach, Hugo Larochelle, Kristen Grauman, Nicolò Cesa-Bianchi, and Roman Garnett (Eds.). 5350–5360.
- [15] Justin Gilmer, Samuel S Schoenholz, Patrick F Riley, Oriol Vinyals, and George E Dahl. 2017. Neural message passing for quantum chemistry. In *ICML*. 1263–1272.
- [16] Michelle Girvan and Mark EJ Newman. 2002. Community structure in social and biological networks. *national academy of sciences* 99, 12 (2002), 7821–7826.
- [17] Daniele Grattarola, Lorenzo Livi, and Cesare Alippi. 2019. Adversarial autoencoders with constant-curvature latent manifolds. *Applied Soft Computing* 81 (2019), 105511.
- [18] Daniele Grattarola, Daniele Zambon, Cesare Alippi, and Lorenzo Livi. 2018. Learning graph embeddings on constant-curvature manifolds for change detection in graph streams. *STAT* 1050 (2018), 16.
- [19] Albert Gu, Frederic Sala, Beliz Gunel, and Christopher Ré. 2019. Learning mixed-curvature representations in product spaces. In *ICLR*.
- [20] Will Hamilton, Zhitao Ying, and Jure Leskovec. 2017. Inductive representation learning on large graphs. In *NeurIPS*. 1024–1034.
- [21] Paul W Holland, Kathryn Blackmond Laskey, and Samuel Leinhardt. 1983. Stochastic blockmodels: First steps. *Social networks* 5, 2 (1983), 109–137.
- [22] Thomas N Kipf and Max Welling. 2016. Variational graph auto-encoders. In *NeurIPS*.
- [23] Thomas N. Kipf and Max Welling. 2017. Semi-Supervised Classification with Graph Convolutional Networks. In *ICLR*.
- [24] Dmitri Krioukov, Fragkiskos Papadopoulos, Maksim Kitsak, Amin Vahdat, and Marián Boguná. 2010. Hyperbolic geometry of complex networks. *Physical Review E* 82, 3 (2010), 036106.
- [25] Jianxin Li, Xingcheng Fu, Hao Peng, Senzhang Wang, Shijie Zhu, Qingyun Sun, Philip S Yu, and Lifang He. 2021. A Robust and Generalized Framework for Adversarial Graph Embedding. *arXiv preprint arXiv:2105.10651* (2021).
- [26] Yaxin Li, Wei Jin, Han Xu, and Jiliang Tang. 2021. Deeprobust: A pytorch library for adversarial attacks and defenses. In *AAAI*.
- [27] Tong Lin and Hongbin Zha. 2008. Riemannian manifold learning. *IEEE transactions on pattern analysis and machine intelligence* 30, 5 (2008), 796–809.
- [28] Yong Lin, Linyuan Lu, and Shing-Tung Yau. 2011. Ricci curvature of graphs. *Tohoku Mathematical Journal, Second Series* 63, 4 (2011), 605–627.
- [29] Fanzhen Liu, Shan Xue, Jia Wu, Chuan Zhou, Wenbin Hu, Cecile Paris, Surya Nepal, Jian Yang, and Philip S. Yu. 2020. Deep Learning for Community Detection: Progress, Challenges and Opportunities. In *IJCAI*. 4981–4987.
- [30] Xiaomei Liu, Suqin Tang, and Jinyan Wang. 2018. Generative Adversarial Graph Representation Learning in Hyperbolic Space. In *CCIR*. 119–131.
- [31] Xiaoxiao Ma, Jia Wu, Shan Xue, Jian Yang, Chuan Zhou, Quan Z Sheng, Hui Xiong, and Leman Akoglu. 2021. A comprehensive survey on graph anomaly detection with deep learning. *IEEE Transactions on Knowledge and Data Engineering* (2021).
- [32] Emile Mathieu, Charline Le Lan, Chris J. Maddison, Ryota Tomioka, and Yee Whye Teh. 2019. Continuous Hierarchical Representations with Poincaré Variational Auto-Encoders. In *NeurIPS*.
- [33] Ujjwal Maulik, Lawrence B Holder, and Diane J Cook. 2006. *Advanced methods for knowledge discovery from complex data*. Springer Science & Business Media.
- [34] Yoshihiro Nagano, Shoichiro Yamaguchi, Yasuhiro Fujita, and Masanori Koyama. 2019. A differentiable gaussian-like distribution on hyperbolic space for gradient-based learning. In *ICML*.
- [35] Hariharan Narayanan and Sanjoy Mitter. 2010. Sample complexity of testing the manifold hypothesis. In *NeurIPS*. 1786–1794.
- [36] Chien-Chun Ni, Yu-Yao Lin, Jie Gao, Xianfeng David Gu, and Emil Saucan. 2015. Ricci curvature of the internet topology. In *INFOCOM*. IEEE, 2758–2766.
- [37] Maximilian Nickel and Douwe Kiela. 2017. Poincaré Embeddings for Learning Hierarchical Representations. In *NeurIPS*. 6338–6347.
- [38] Yann Ollivier. 2009. Ricci curvature of Markov chains on metric spaces. *Journal of Functional Analysis* 256, 3 (2009), 810–864.
- [39] Fragkiskos Papadopoulos, Maksim Kitsak, M Ángeles Serrano, Marián Boguná, and Dmitri Krioukov. 2012. Popularity versus similarity in growing networks. *Nature* (2012), 537–540.
- [40] Hao Peng, Ruitong Zhang, Yingdong Dou, Renyu Yang, Jingyi Zhang, and Philip S Yu. 2021. Reinforced neighborhood selection guided multi-relational graph neural networks. *ACM Transactions on Information Systems (TOIS)* 40, 4 (2021), 1–46.
- [41] Hao Peng, Ruitong Zhang, Shaoning Li, Yuwei Cao, Shirui Pan, and Philip Yu. 2022. Reinforced, Incremental and Cross-lingual Event Detection From Social Messages. *IEEE Transactions on Pattern Analysis and Machine Intelligence* (2022).
- [42] Salah Rifai, Yann N Dauphin, Pascal Vincent, Yoshua Bengio, and Xavier Muller. 2011. The manifold tangent classifier. In *NeurIPS*, Vol. 24. 2294–2302.
- [43] Prithviraj Sen, Galileo Namata, Mustafa Bilgic, Lise Getoor, Brian Galligher, and Tina Eliassi-Rad. 2008. Collective classification in network data. *AI magazine* 29, 3 (2008), 93–93.
- [44] Jayson Sia, Edmond Jonckheere, and Paul Bogdan. 2019. Ollivier-ricci curvature-based method to community detection in complex networks. *Scientific reports* 9, 1 (2019), 1–12.
- [45] Ondrej Skopek, Octavian-Eugen Ganea, and Gary Bécigneul. 2020. Mixed-curvature Variational Autoencoders. In *ICLR*.
- [46] Xing Su, Shan Xue, Fanzhen Liu, Jia Wu, Jian Yang, Chuan Zhou, Wenbin Hu, Cécile Paris, Surya Nepal, Di Jin, Quan Z. Sheng, and Philip S. Yu. 2021. A Comprehensive Survey on Community Detection with Deep Learning. *CoRR abs/2105.12584* (2021).
- [47] Li Sun, Zhongbao Zhang, Junda Ye, Hao Peng, Jiawei Zhang, Sen Su, and Philip S Yu. 2021. A Self-supervised Mixed-curvature Graph Neural Network. *arXiv preprint arXiv:2112.05393* (2021).
- [48] Li Sun, Zhongbao Zhang, Jiawei Zhang, Feiyang Wang, Yang Du, Sen Su, and S Yu Philip. 2020. PERFECT: A Hyperbolic Embedding for Joint User and Community Alignment. In *ICDM*. IEEE, 501–510.
- [49] Li Sun, Zhongbao Zhang, Jiawei Zhang, Feiyang Wang, Hao Peng, Sen Su, and Philip S Yu. 2021. Hyperbolic Variational Graph Neural Network for Modeling Dynamic Graphs. In *AAAI*.
- [50] Qingyun Sun, Jianxin Li, Hao Peng, Jia Wu, Xingcheng Fu, Cheng Ji, and Philip S Yu. 2022. Graph Structure Learning with Variational Information Bottleneck. In *AAAI*.
- [51] Qingyun Sun, Jianxin Li, Hao Peng, Jia Wu, Yuanxing Ning, Philip S Yu, and Lifang He. 2021. Sugar: Subgraph neural network with reinforcement pooling and self-supervised mutual information mechanism. In *Web Conference*. 2081–2091.
- [52] Qingyun Sun, Hao Peng, Jianxin Li, Senzhang Wang, Xiangyu Dong, Liangxuan Zhao, S Yu Philip, and Lifang He. 2020. Pairwise learning for name disambiguation in large-scale heterogeneous academic networks. In *ICDM*. IEEE, 511–520.
- [53] Alexandru Tifrea, Gary Bécigneul, and Octavian-Eugen Ganea. 2019. Poincaré Glove: Hyperbolic Word Embeddings. In *ICLR*.
- [54] Abraham A Ungar. 1999. The hyperbolic Pythagorean theorem in the Poincaré disc model of hyperbolic geometry. *The American mathematical monthly* 106, 8 (1999), 759–763.
- [55] Abraham A Ungar. 2005. *Analytic hyperbolic geometry: Mathematical foundations and applications*. World Scientific.
- [56] Abraham Albert Ungar. 2008. A gyrovector space approach to hyperbolic geometry. *Synthesis Lectures on Mathematics and Statistics* 1, 1 (2008), 1–194.
- [57] Abraham Albert Ungar. 2014. *Analytic hyperbolic geometry in n dimensions: An introduction*. CRC Press.
- [58] Petar Velickovic, William Fedus, William L. Hamilton, Pietro Lio, Yoshua Bengio, and R. Devon Hjelm. 2019. Deep Graph Infomax. In *ICLR*.
- [59] Hongwei Wang, Jia Wang, Jialin Wang, Miao Zhao, Weinan Zhang, Fuzheng Zhang, Xing Xie, and Minyi Guo. 2018. Graphgan: Graph representation learning with generative adversarial nets. In *AAAI*. 2508–2515.
- [60] Shen Wang, Xiaokai Wei, Cicero dos Santos, Zhiguo Wang, Ramesh Nallapati, Andrew Arnold, Bing Xiang, and Philip S. Yu. 2020. H2KGAT: Hierarchical Hyperbolic Knowledge Graph Attention Network. In *EMNLP*. 4952–4962.
- [61] Duncan J Watts and Steven H Strogatz. 1998. Collective dynamics of ‘small-world’ networks. *Nature* 393, 6684 (1998), 440–442.
- [62] Thomas James Willmore. 2013. *An introduction to differential geometry*. Courier Corporation.

- [63] Richard C Wilson, Edwin R Hancock, Elzbieta Pekalska, and Robert PW Duin. 2014. Spherical and hyperbolic embeddings of data. *IEEE transactions on pattern analysis and machine intelligence* 36, 11 (2014), 2255–2269.
- [64] Jia Wu, Xingquan Zhu, Chengqi Zhang, and Zhihua Cai. 2013. Multi-instance Multi-graph Dual Embedding Learning. In *ICDM*. 827–836.
- [65] Jiacheng Xu and Greg Durrett. 2018. Spherical latent spaces for stable variational autoencoders. *EMNLP* (2018).
- [66] Ze Ye, Kin Sum Liu, Tengfei Ma, Jie Gao, and Chao Chen. 2019. Curvature graph network. In *ICLR*.
- [67] Wenchao Yu, Cheng Zheng, Wei Cheng, Charu C Aggarwal, Dongjin Song, Bo Zong, Haifeng Chen, and Wei Wang. 2018. Learning deep network representations with adversarially regularized autoencoders. In *SIGKDD*. 2663–2671.
- [68] Shijie Zhu, Jianxin Li, Hao Peng, Senzhang Wang, and Lifang He. 2021. Adversarial Directed Graph Embedding. In *AAAI*, Vol. 35. 4741–4748.
- [69] Arkaitz Zubiaga, Ahmet Aker, Kalina Bontcheva, Maria Liakata, and Rob Procter. 2018. Detection and resolution of rumours in social media: A survey. *ACM Computing Surveys (CSUR)* 51, 2 (2018), 1–36.